



King Saud University
Arabian Journal of Chemistry

www.ksu.edu.sa
www.sciencedirect.com



ORIGINAL ARTICLE

Microwave radiation hydrothermal synthesis and characterization of micro- and mesoporous composite molecular sieve Y/SBA-15

Wenyuan Wu *, Chunwei Shi, Bian Xue, Bai Yuting

School of Material and Metallurgy, Northeastern University, Shenyang 110819, Liaoning, China

Received 11 September 2013; accepted 26 October 2013

KEYWORDS

Y/SBA-15;
Micro- and mesoporous
composite molecular sieve;
Method of crystal growth;
Microwave radiation hydro-
thermal synthesis

Abstract A microwave radiation hydrothermal method to control synthesis of micro- and mesoporous Y/SBA-15 composite molecular sieves was reported. The synthesized SBA-15 and Y/SBA-15 were characterized by scanning electron microscopy (SEM) and N₂ adsorption–desorption. The three kinds of different concentrations of hydrochloric acid (0.75 M, 2 M and 3.25 M) were used to investigate the effect on Y/SBA-15. The analysis results of the composite products indicated that the optimization synthesis condition employed zeolite type Y and TEOS as silicon sources under 0.75 M hydrochloric acid by the microwave radiation hydrothermal synthesis method. The N₂ adsorption–desorption test results of micro–mesoporous composite molecular sieve type Y/SBA-15 in mesoporous extent indicated that SBET is 355.529 m²/g, \overline{D}_{BET} is 4.050 nm, and mesoporous aperture focuses on the distribution region of 5.3 nm. It was found that the received composite product has an appropriate proportion of smaller size, larger size pore structure and the thicker pore wall. In addition, its internal channels have a high degree of order and smooth flow in long-range channels.

Crown Copyright © 2013 Published by Elsevier Ltd. All rights reserved.

1. Introduction

Microporous molecular sieves have been extensively used in acid catalysis due to their unique pore structures and strong intrinsic acidities. Unfortunately, small pore size of such

microporous materials hinders their application in catalytic reactions involving large molecules. Since the early 1990s, mesoporous molecular sieves have attracted considerable attention owing to their potential use for the conversion of large molecules (Kresge et al., 1992; Zhang et al., 1999; Zhao et al., 1998). However, the practical application is still limited due to their relatively low acidity and thermal stability arising from the amorphous character of the pore walls (Beck et al., 1992). Thus, there is great interest in the synthesis of hierarchically structured composite materials which combine the performances of both mesoporous and microporous molecular sieves. A lot of researches have been devoted into the synthesis and characterization of micro- and mesoporous materials

* Corresponding author. Tel./fax: +86 24 8368 3016.
E-mail address: wuwenyuan2013@gmail.com (W. Wu).

Peer review under responsibility of King Saud University.



Production and hosting by Elsevier

during the last decades (Zakaria and Mohamed, 2004; Chen et al., 2003).

Microporous zeolite type Y, traditional catalytic and adsorption material, has smaller aerodynamic aperture, in particular, the size of the reactant is limited to about 1.2 nm below, which limits the size and shape of reactant infiltrating in the mesh of catalyst skeleton, and affects the selection of catalytic reaction. Though the aperture size of mesoporous molecular sieve type SBA-15 is uniform and adjustable, SBA-15 has poorer hydrothermal stability and lower catalytic activity center as compared with zeolite type Y because the pore channels of SBA-15 are thinner and amorphous. So the catalytic cracking effect on polyolefin macromolecule of microporous zeolite type Y and mesoporous molecular sieves type SBA-15 is not quite ideal.

Y/SBA-15 combines the advantages of zeolite type Y and mesoporous molecular sieves type SBA-15. It has the pore channel advantages of mesoporous materials, strong acid and high hydrothermal stability of microporous zeolite type Y at the same time. The two model frames, microporous and mesoporous, had complemented advantages and synergic effects. Thus the larger mesoporous can provide access for macromolecular reaction, while the part or complete crystallization of the pore wall can provide possibility for the shape-selective catalytic of small molecule and stronger acid center catalytic of macromolecules.

2. Experimental set-up

Microporous zeolite type Y is synthesized. The molar ratio of $\text{SiO}_2:\text{Al}_2\text{O}_3:\text{Na}_2\text{CO}_3:\text{H}_2\text{O}$ (9:1:3:120) was applied, and then it was left for 24 h. The solution was hydrothermally treated under microwave conditions at 120 °C for 1 min using a constant heating power of 800 W, and then it was hydrothermally treated under microwave conditions at 100 °C for 20 min using a constant heating power of 200 W. The products, thereafter, were crash-cooled, isolated by filtration, washed several times with demineralized water, and dried in air for 3 h at 120 °C (Arafat et al., 1993).

SBA-15 is synthesized. The block copolymer P123 (BASF) was used as the active surfactant for mesoporous silica SBA-15 with good reproducibility. Four grams of P123 was dissolved into 30 g of water and 120 g of certain concentration of HCl under vigorous stirring at 40 °C. After the mixture was clear, 9.5 g of tetraethylorthosilicate (TEOS) was poured into the solution with continued stirring. Then it was hydrothermally treated under microwave conditions at 100 °C for 2 h. The

product was filtered, washed, dried at 110 °C and calcined at 560 °C for 5 h (Newalkar et al., 2003).

Y/SBA-15 is synthesized. Four grams of P123 was dissolved into 30 g of water under vigorous stirring at 40 °C. After the mixture became clear, 9.5 g of tetraethylorthosilicate (TEOS) was poured into the solution with continued stirring. Microporous zeolite type Y (4.0 g) and 120 g of certain concentration of HCl were placed in the solution with continued stirring. Then it was hydrothermally treated under microwave conditions at 100 °C for 2 h using a constant heating power of 600 W. The product was filtered, washed, dried at 110 °C and calcined at 550 °C for 6 h. Internal channels have a high degree of order and smooth flow in long-range channels.

3. Results and discussion

3.1. Electron microscopy

SEM images were recorded using a Hitachi SSX-550 with an acceleration voltage of 15 kV. The samples were mounted using a conductive carbon double-sided sticky tape. A thin coating of gold sputter was deposited onto the samples to reduce the effects of charging.

SEM photos of microporous zeolite type Y are shown in Fig. 1. The photograph of zeolite Y exhibits small uniformly sized crystal aggregates with a maximum crystal size of 2 μm , indicating simultaneous and abundant nucleation. Investigations on the crystallization of faujasite-type zeolites show that nucleation occurs only in a restricted area of compositions in conventional heating.

Fig. 2 displays the SEM images of synthesized SBA-15. The sample (a) (0.75 M) has abundant stick particles with 0.05–0.1 μm sizes, while, it clearly illustrates the tunnel-like structure of SBA-15. The aperture size of mesoporous molecular sieve type SBA-15 is uniform and adjustable. When the concentration of hydrochloric acid rises to 3.25 M mesoporous molecular sieve type SBA-15 with gobbets appears, while the mesoporous phase still remains. It has the loose and coarse face with a thin layered structure aggregates.

As shown in Fig. 3, sheet-like crystals of zeolite Y and mesoporous molecular sieve type SBA-15 cannot be found. The SEM images show that both microporous and mesoporous dual-distribution model frames consist in the samples at the same time. And the proportion of microporous and mesoporous is moderate. The sample (a) (0.75 M) has plentiful stick particles with equality of 0.2 μm size which was larger than the size of type SBA-15. The sample synthesizes with a low

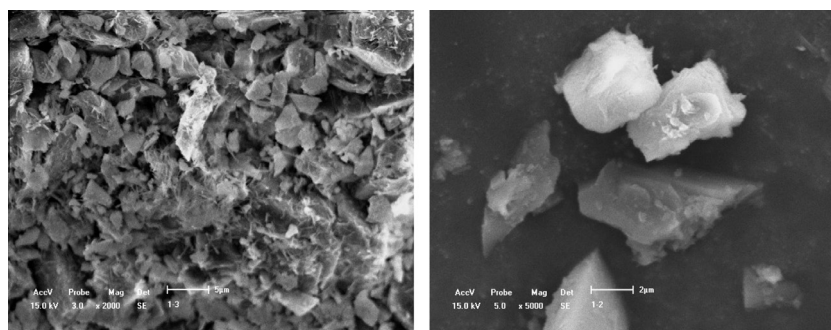


Figure 1 SEM photos of microporous zeolite type Y.

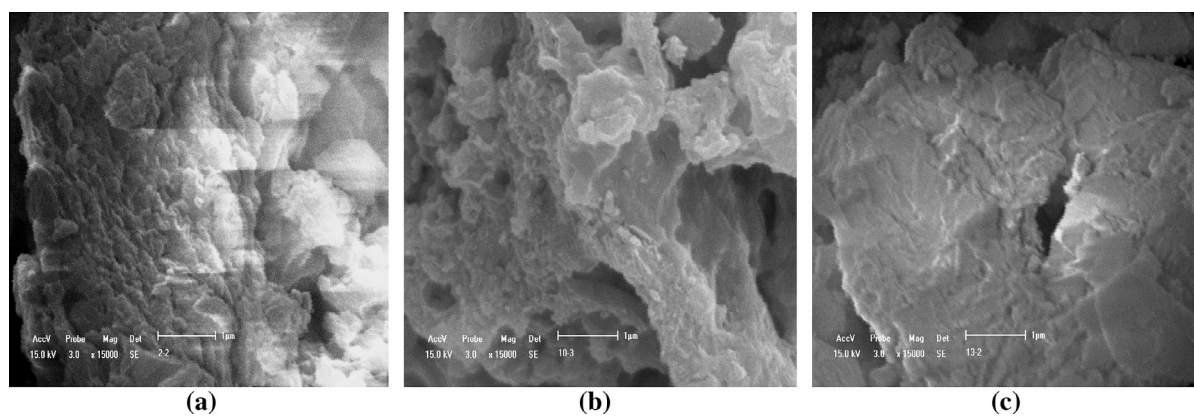


Figure 2 SEM photos of mesoporous molecular sieve type SBA-15 with different concentrations of hydrochloric acid (a) 0.75 M, (b) 2 M and (c) 3.25 M.

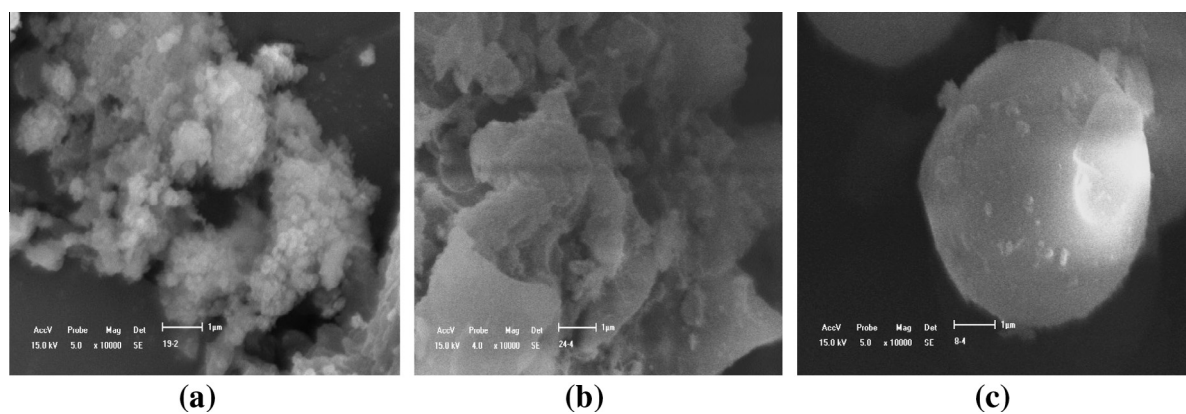


Figure 3 SEM photos of micro-mesoporous molecular sieve type Y/SBA-15 with different concentrations of hydrochloric acid (a) 0.75 M, (b) 2 M and (c) 3.25 M.

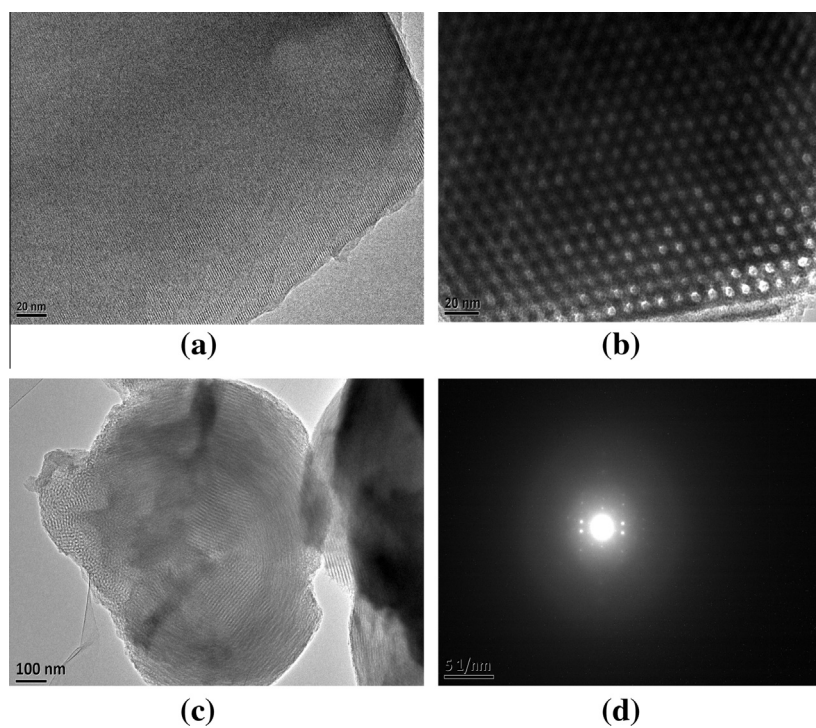
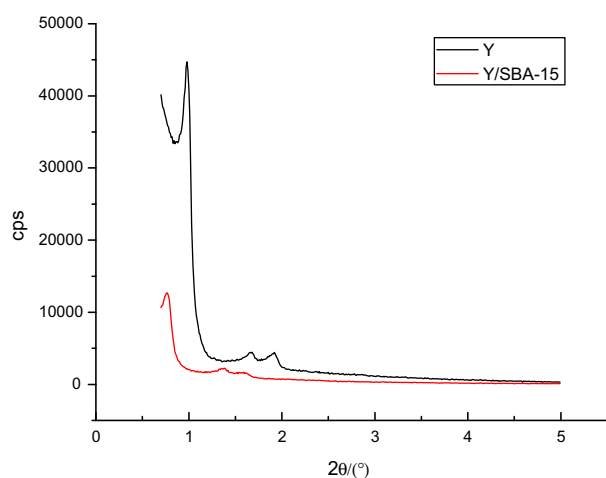


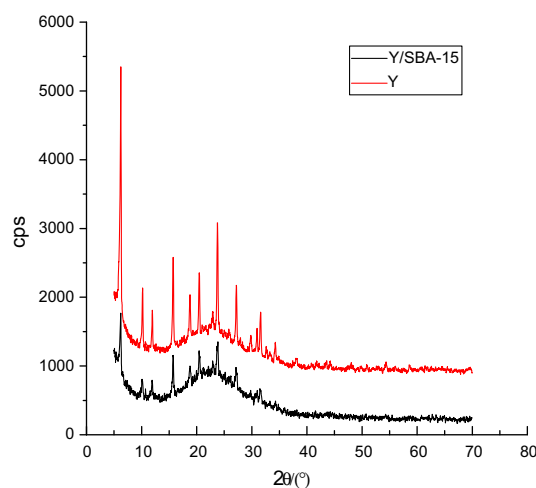
Figure 4 TEM photos of Y, SBA-15 and Y/SBA-15.

concentration of hydrochloric acid having a smooth face and even granular structure aggregates. With the concentration of hydrochloric acid raised to 3.25 M, the diameter of type Y/SBA-15 increases to 4–5 μm . It is composed of smooth-faced spherical particles. HCl played a role of catalyst in the synthesizing process. It could enhance the formation of hexagonal ordered arrangement of the surfactant micelles (Zhao et al., 2006).

TEM images of calcined Y, SBA-15 and Y/SBA-15 are shown in Fig. 4. The average wall thick of 1.8 nm and 7 nm can be calculated from the scale bar (Fig. 4a and b). The average wall thick of 25 nm and 1.5 nm can be calculated from the scale bar (Fig. 4d). Mesoporous aperture and the aperture size meet the requirements of the standard in the composite molecular sieve. Fig. 3(c) shows that microporous and mesoporous composite molecular sieves present round ball. The round ball's internal structure is shown in Fig. 4(c). The microporous structure is inside, and the mesoporous structure is surrounded in the external. Electron microscopy proves that the synthesis of composite molecular sieves has microporous and mesoporous channels at the same time. The compound that



(a) the small angle XRD spectra



(b) wide-angle XRD spectra

Figure 5 The XRD spectra of Y, SBA-15 and Y/SBA-15.

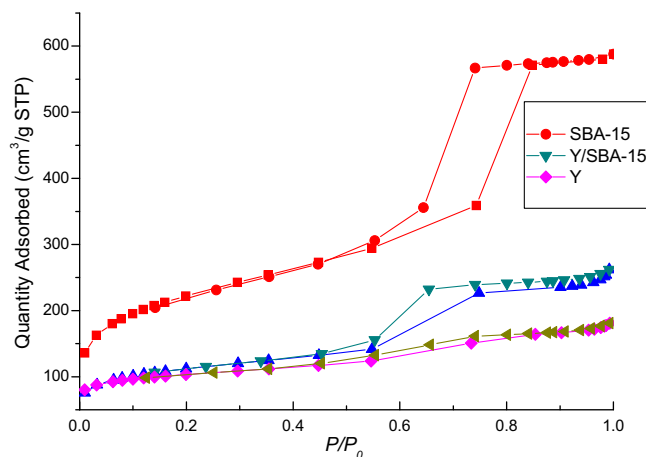


Figure 6 Y, SBA-15 and Y/SBA-15 adsorption-desorption isotherms.

we synthesized is not a single microporous molecular sieve but a mechanical mixture of mesoporous molecular sieves.

3.2. Powder XRD analysis

Fig. 5(a) shows small angle of the sample appear the six party system (100), (110), (200) crystal plane characteristic diffraction peaks. The preparation of SBA-15 is highly ordered two-dimensional six corner structure. The strength of the characteristic peak of Y/SBA-15 decreased, probably because the pore is introduced in the Y molecular sieve and the zeolite crystallinity when pure mesoporous molecular sieve decreased. Fig. 5(b) shows, WXR curve of Y/SBA-15 WXR curve and Y and SBA-15 are different, but also not the simple superposition of Y and SBA-15 curve. The mechanical mixing sample hydrothermal synthesis of Y/SBA-15 microporous mesoporous composite material is not Y and SBA-15. d_{100} is 5.41 nm, a is 6.25 nm, and the thickness of pore wall is 2.2 nm.

Analysis of N_2 adsorption-desorption Y, SBA-15, Y/SBA-15 adsorption-desorption isotherms is shown in Fig. 6.

It can be seen from Fig. 6, the Y adsorption-desorption isotherms for I, microporous molecular sieve is a typical line;

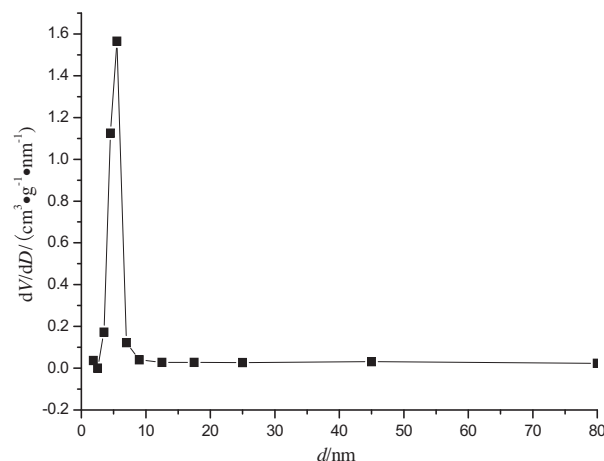


Figure 7 The pore size distribution of Y/SBA-15.

Table 1 BET surface area, BJH average desorption pore volume, BET average pore diameter, BJH average adsorption and desorption pore diameters of Y/SBA-15.

Sample	SBET [m ² g ⁻¹]	$V_{BJHDesorption}$ [cm ³ g ⁻¹]	\overline{D}_{BET} [nm]	$\overline{D}_{BJHAdsorption}$ [nm]	$V_{BJHDesorption}$ [nm]
Y/SBA-15 (0.75 M)	355.529	0.351	4.050	5.739	5.363
Y/SBA-15 (2 M)	73.196	0.225	10.900	9.964	8.255
Y/SBA-15 (3.25 M)	135.480	0.167	4.495	3.842	3.678

adsorption – desorption isotherms for SBA-15 type V is mesoporous molecular sieve type typical line, Y/SBA-15 IV line is typical at low relative pressure stage, when the relative pressure $P/P_0 < 0.1$, desorption and adsorption branch fully coincide, the adsorption quantity of P/P_0 increases linearly with increased significantly. When the relative pressure at $0.1 < P/P_0 < 0.35$ range, the adsorption capacity with the increase of P/P_0 also increased linearly, but increase the adsorption capacity of N₂ than that of $P/P_0 < 0.1$ relatively gentle, this is because the pressure is relatively low N₂ in the mesoporous surface monolayer dispersion caused by. At low relative pressure stage, when the relative pressure increases further, the $P/P_0 > 0.35$, the adsorption curve upward, which is generated in the capillary N₂ mesoporous enclosed frame aggregation results, due to the capillary condensation of N₂ molecules filled mesoporous, adsorption with P/P_0 increased significantly, the curve of adsorption jump. It can be seen from Fig. 7, the mechanical mixing sample hydrothermal synthesis of Y/SBA-15 microporous mesoporous composite material is not Y and SBA-15, and the thickness of pore wall is 6.2 nm.

As shown in Table 1, the N₂ adsorption–desorption test results of micro–mesoporous composite molecular sieve type Y/SBA-15 in mesoporous extent indicate that SBET is 355.529 m²/g, \overline{D}_{BET} is 4.050 nm, and mesoporous aperture focuses on the distribution region of 5.3 nm.

4. Conclusions

This study explored a microwave radiation hydrothermal synthesis of the microporous zeolite type Y, mesoporous molecular sieve type SBA-15, and micro- and mesoporous composite molecular sieve Y/SBA-15. The material structure strongly depends on the conditions used, which is confirmed by SEM,

SXRD and gas N₂ adsorption results. The successful synthesis of Y/SBA-15 with the high-rate synthesis method, not only created hope to the better catalytic cracking effect of polyolefins but also laid a solid foundation for the condition control, process development and industrialization on the high-rate synthesis of Y/SBA-15.

Acknowledgements

This work was financially supported by the National Natural Science Foundation of China (51274060).

References

- Arafat, A., Jansen, J.C., Ebaid, A.R., 1993. Zeolites 13, 162–165.
- Beck, J.S., Vartuli, J.C., Roth, W.J., Leonowicz, M.E., Kresge, C.T., Schmitt, K.D., Chu, C.T.W., Olson, D.H., Sheppard, E.W., McCullen, S.B., Higgins, J.B., Schlenker, J.L., 1992. J. Am. Chem. Soc. 114, 10834–10843.
- Chen, H.L., Shen, B.J., Pan, H.F., 2003. Chem. Lett. 32, 726–727.
- Kresge, C.T., Leonowicz, M.E., Roth, W.J., Beck, J.S., 1992. Nature 359, 710–712.
- Newalkar, B.L., Choudary, N.V., Turaga, U.T., 2003. Chem. Mater. 15, 1474–1479.
- Zakaria, R., Mohamed, A.R., 2004. Appl. Catal. A 274, 15–23.
- Zhang, W., Pauly, T.R., Pinnavaia, T.J., 1999. Chem. Mater. 9, 2491–2498.
- Zhao, D., Feng, J., Huo, Q., Melosh, N., Fredrickson, G.H., Chmelka, B.F., Stucky, G.D., 1998. Science 279, 548–552.
- Zhao, C.X., Chen, W., Liu, Q., Tian, G., 2006. Acta Phys. Chim. Sin. 22, 1201–1205.